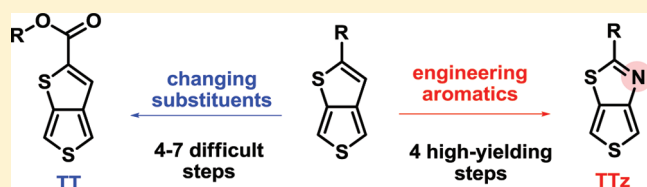


## Improved Synthesis of Thienothiazole and Its Utility in Developing Polymers for Photovoltaics

Rycel Uy,<sup>†</sup> Liqiang Yang,<sup>‡</sup> Huaxing Zhou,<sup>†</sup> Samuel C. Price,<sup>†</sup> and Wei You<sup>\*,†,‡</sup><sup>†</sup>Department of Chemistry, University of North Carolina at Chapel Hill, Chapel Hill, North Carolina 27599-3290, United States<sup>‡</sup>Curriculum in Applied Sciences and Engineering, University of North Carolina at Chapel Hill, Chapel Hill, North Carolina 27599-3287, United States

## Supporting Information

**ABSTRACT:** In response to the structural and electronic limitations of the popular benzo[1,2-*b*:4,5-*b'*]dithiophene–thieno[3,4-*b*]thiophene (PBnDT–TT) polymer series, this study explores the design and synthesis of a thienothiazole (TTz) moiety. The synthesis of TTz was streamlined down to four high-yielding steps, resulting in the new polymer PBnDT–TTz for organic solar cells. By incorporating TTz, a nitrogen is directly introduced into the polymer backbone which tunes the HOMO level and eliminates the reliance on external substituents. Compared to its TT analogue, PBnDT–TTz exhibits the same HOMO level of  $-5.06$  eV and the same  $V_{oc}$  of  $0.69$  eV, yet a higher power conversion efficiency of 2.5%. These promising results demonstrate the benefits of backbone modification and the great potential of TTz in the design of new polymers for organic photovoltaics.



## INTRODUCTION

Although substantial improvements have been made in the development of donor polymers for organic solar cells<sup>1–5</sup> reaching over 5% power conversion efficiency,<sup>6–12</sup> recent years have seen only incremental advances. This highlights the need to probe the inherent issues limiting current donor materials and focus on discovering design fundamentals necessary to develop better-performing polymers. Currently, one of the top performers is a polymer series consisting of alternating benzo[1,2-*b*:4,5-*b'*]dithiophene (BnDT) and thieno[3,4-*b*]thiophene (TT) moieties that have reached efficiencies over 7%.<sup>13–18</sup>

The success of the PBnDT–TT series can be attributed to this material meeting four of the five generally accepted criteria necessary for donor polymers to perform well in bulk heterojunction (BHJ) solar cells.<sup>16,19–22</sup> Because the TT moiety can stabilize its quinoidal form, this leads to more double-bond character in the polymer backbone which leads to (1) a low band gap of  $\sim 1.5$  eV and (2) high hole mobility. Also, since every BnDT–TT unit contains three solubilizing side groups, the alkyl chains need not be excessively long. Moderate chain lengths not only allow PBnDT–TT to achieve (3) good solubility in spin-casting solvents and (4) high molecular weight<sup>23,24</sup> but also help to enhance short circuit current ( $J_{sc}$ ).<sup>25</sup> However, even with an electron-withdrawing ester as the stabilizing group, the electron-rich nature of TT raises the highest occupied molecular orbital (HOMO) level too high at about  $-5.0$  eV,<sup>14,26</sup> failing to achieve (5) a low-lying HOMO level around  $-5.4$  eV and leading to lower open circuit voltage ( $V_{oc}$ ) and therefore lower efficiency.<sup>3,21</sup>

In an effort to lower the HOMO level of the polymer, TT has been substituted with various electron-withdrawing groups. For

example, Hou et al. replaced the ester with a ketone but observed almost no change in the HOMO level.<sup>15</sup> Similarly, when fluorine was placed on TT, this lowered the HOMO level by only 0.11 eV.<sup>14</sup> When Huang et al. used the even more electronegative sulfonyl on TT instead, the resulting HOMO level was still very similar.<sup>17</sup> Although adding and changing substituents has shown some success, directly engineering the polymer backbone is a more effective method to tune energy levels.<sup>22,27</sup> Given that further structural modifications to TT have been nearly exhausted, a new unit needs to be designed that still incorporates the advantages of TT while offering similar or lower HOMO levels in its polymers.

One way to increase the electron-deficiency of TT and eliminate the need for external ester or fluorine substituents is to introduce an electron-deficient unit such as thiazole. This will change the thienothiophene (TT) to thienothiazole (TTz), which is also capable of stabilizing its quinoid form.<sup>28</sup> To gauge the effect on the HOMO level, density functional theory (DFT) calculations were collected for alkylated TTz and TTs with an alkyl or an ester alkyl chain (Figure 1). All three were paired with BnDT<sup>29,30</sup> since this unit has demonstrated numerous favorable results in BHJ solar cells.<sup>10,16</sup> As shown in Table 1, calculations predict that adding the ester to the TT versus changing the carbon to nitrogen (TTz) lower the HOMO level by a similar amount, 0.15 and 0.14 eV, respectively. Thus, in this initial study we want to investigate how the TTz-based polymer's solar cell performance will compare with that of the ester TT-based polymer.

Received: August 10, 2011

Revised: September 27, 2011

Published: November 03, 2011

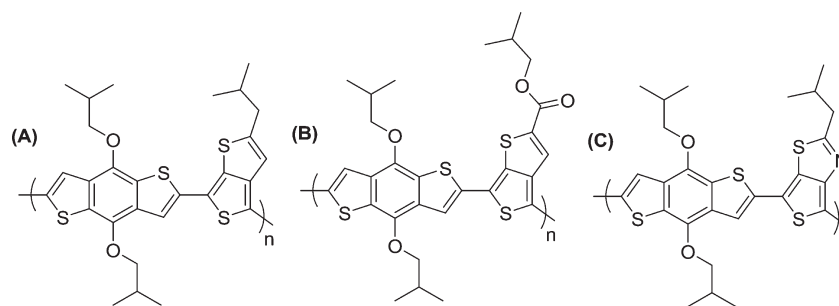


**Figure 1.** Oligomeric units of (A) alkyl TT, (B) ester TT, and (C) alkyl TTz used to perform DFT calculations.

**Table 1.** DFT Calculations for BnDT Copolymerized with Alkylated TT, Ester TT, and Alkylated TTz

	HOMO [eV]	LUMO [eV]	$E_g$ [eV]
alkyl TT	−5.06	−1.75	3.31
ester TT	−5.21	−2.17	3.04
alkyl TTz	−5.20	−1.86	3.34

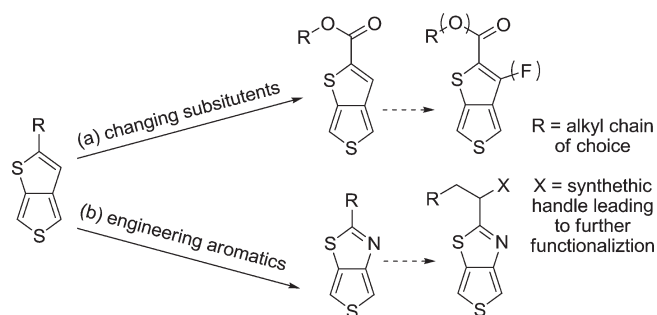


**Figure 2.** Two different approaches to tune the energy levels of thienothiophene, where dashed arrows indicate further structural variations.

In addition to a similar HOMO level, TTz possesses several potential improvements over ester TT. The unfunctionalized  $\alpha$ -position provides a synthetic handle for further modifications that would allow for further lowering of the HOMO level (Figure 2). To date, there had only been one previous report of thienothiophene in the literature,<sup>28</sup> which involved seven mostly low-yielding steps. This procedure was recently reproduced by Leclerc and co-workers during the preparation of this paper, and the reported yields were similarly low.<sup>31</sup> If the number of steps could be drastically shortened, TTz would also be synthetically favorable over TT which can take four to seven steps, each rendition reported as being difficult and costly.<sup>14,15,17,18,32</sup> These synthetic challenges with TT will hinder this material's viability of being reproduced on a commercial scale in the future.

Herein we report a new, facile synthetic route to TTz, involving only four high-yielding steps. To make TTz, the key bond disconnection is the C–S bond in the top thiazole ring rather than the C–S–C bond formation toward the bottom thiophene unit, allowing us to make the unit much faster. From this optimized route, a new polymer PBnDT–TTz was made and its properties were studied alongside its TT analogue. Compared to PBnDT–TT, PBnDT–TTz exhibits better surface morphology, hole mobility,  $J_{sc}$  and thus higher solar cell efficiency (2.3% over 1.2%), demonstrating the great potential of this new structural moiety (TTz) in organic photovoltaics.

## RESULTS AND DISCUSSION

**Synthesis of Thienothiophene Monomer and Polymer.** The originally published procedure<sup>28</sup> was reproduced on a test run using an undecyl alkyl chain with the following yields shown in Scheme 1. As can be seen, this synthetic route suffers from several drawbacks. The most significant one is that the chain length must be decided in the first step, making later structural modifications to TTz inefficient and tedious. Furthermore, seven steps are required to get to TTz, many of which are low-yielding, especially in the later steps forming the thiophene ring.

Rather than starting with thiazole and attempting to form the second thiophene ring, we decided that starting with the thiophene ring would be more advantageous, since a variety of functionalized thiophenes are commercially available. Additionally, carbon–heteroatom bond disconnections allow for a much faster synthesis and a broader scope of reactions to be considered.<sup>33</sup> Thus, we decided to construct the thiazole from an amide at the 3-position of the thiophene and then close the ring via Cu-catalyzed cyclization between the carbon–sulfur bond.<sup>34</sup> Functionalizing the thiophene with an amide at this position provides us with a number of benefits (Figure 3). It allows us to anchor on our desired alkyl chain, which can later be converted to a thioamide easily, and there are a multitude of amide precursors we can start from such as a nitro group, azide, amine, carboxylic acid, etc.

We chose to begin with a carboxylic acid and mapped out an alternate synthetic route (Scheme 2). However, 3-bromothiophene-4-carboxylic acid (**1**) itself could not be generated pure and in high yield. Solvent choice played an important role in this halogen–lithium exchange reaction. Tetrahydrofuran could not be used since 3,4-dibromothiophene can undergo scrambling in this solvent.<sup>35</sup> When hexanes was used, the desired carboxylic acid was isolated but in low yield since 3,4-dibromothiophene is only sparingly soluble in hexanes at low temperatures. There was no solubility issue when diethyl ether was used as the solvent, and furthermore, deuterium-labeling experiments proved that scrambling of the starting material did not occur in this solvent. However, this reaction in diethyl ether led to the dicarboxylic acid as the major product (Figure 4), most likely because 3-bromothiophene-4-carboxylic acid is more reactive toward halogen–lithium exchange than 3,4-dibromothiophene.

A third route shown in Scheme 3 was then proposed. Rather than synthesizing a *boc*-protected amine and then deprotecting to attach the alkyl chain as was originally suggested in Scheme 2, we decided to make 3-azido-4-bromothiophene<sup>36</sup> and reduce it to the free amine (**2**) in one pot. The corresponding acid chloride is then added to attach the alkyl chain of choice (ethylhexyl) to

Scheme 1. Synthesis of Thienothiazole, Procedure I, Reproduction of Literature Procedure with Observed Yields

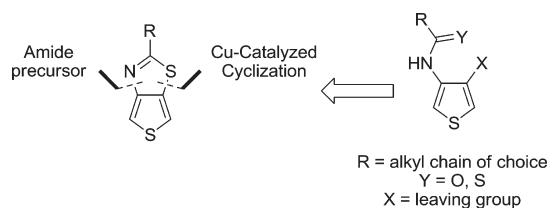
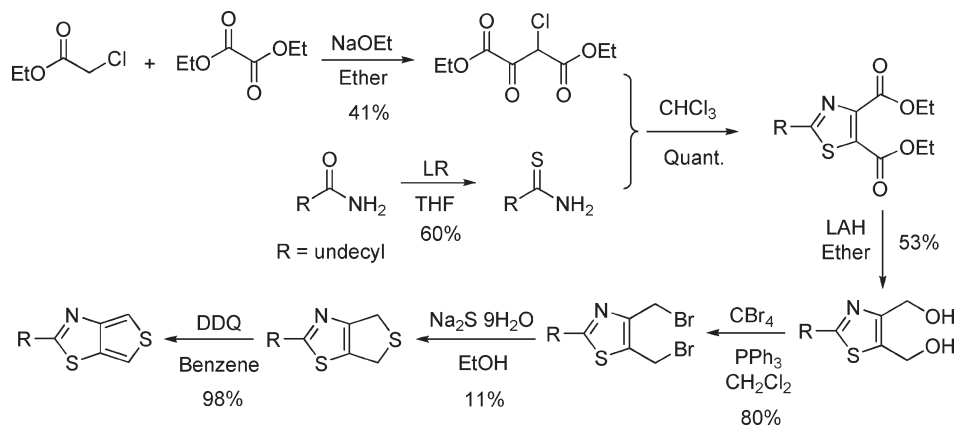
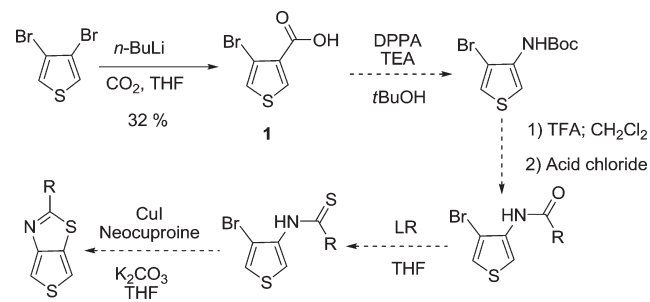


Figure 3. Retrosynthetic analysis of thienothiazole.

Scheme 2. Synthesis of Thienothiazole, Procedure II, via 3-Bromothiophene-4-carboxylic Acid



obtain our amide (3). Particularly noteworthy in this synthesis is the Cu-catalyzed cyclization<sup>34</sup> of the thioamide (4), which was adapted from a procedure reported by Evindar et al.<sup>34</sup> This C–S bond forming reaction is very clean, proceeds in quantitative yield, and has previously been demonstrated as an efficient way to form benzothiazoles<sup>34</sup> and now thienothiazoles as well. Procedure III was our first successful synthesis of TTz and was an improvement over the previous two routes in that the yields were higher and that it afforded the target compound in only five steps.

In order to further optimize the route, we decided to isolate 3-azido-4-bromothiophene instead and treat it with the appropriate carboxylic acid to attach the alkyl chain of choice (ethylhexyl). This reaction is known as the Staudinger–Vilarrasa reaction,<sup>37</sup> which allows us to synthesize our desired amide from the azide in one step. This synthetic route (Scheme 4) is a dramatic improvement over the previous methods since it has only four steps, yields are higher, and the chain length is introduced much later in the synthesis. TTz is then brominated via *N*-bromosuccinimide (NBS) (5) and

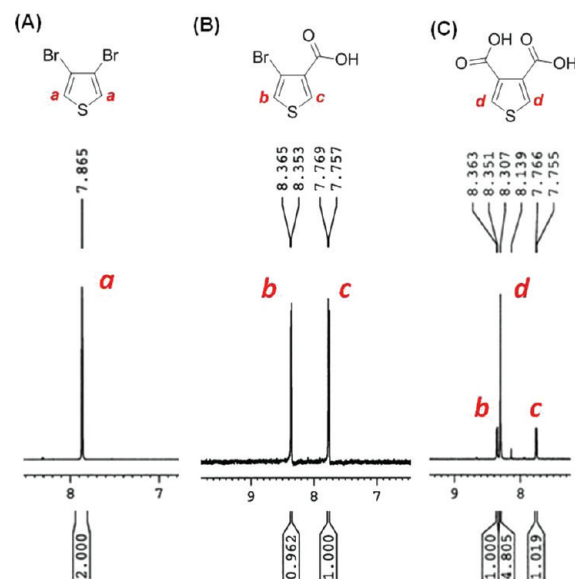


Figure 4. Proton NMR spectra of (A) 3,4-dibromothiophene, (B) 3-bromothiophene-4-carboxylic acid, and (C) 3,4-dicarboxylic acid thiophene.

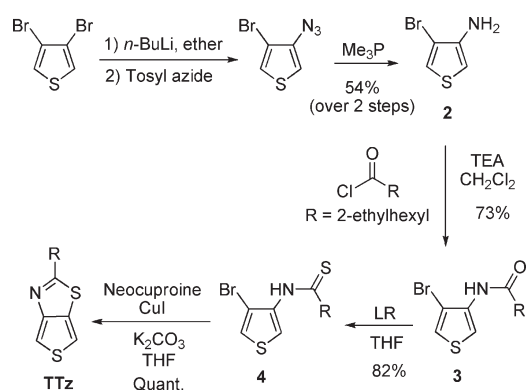
polymerized via Stille polycondensation<sup>38,39</sup> with the corresponding benzodithiophene distannane monomer (BnDT) using conventional heating conditions to afford the new PBnDT–TTz polymer (Scheme 5).

For the sake of comparison, the analogous TT polymer was also synthesized according to the literature<sup>14</sup> since the photovoltaic (PV) properties of this specific BnDT–TT polymer with ethylhexyl chains on both units had not been previously reported. Both polymers were purified by Soxhlet extraction with methanol, ethyl acetate, hexanes, and chloroform. Using the resulting solids from the chloroform fraction, the molecular weights of the polymers were determined by high-temperature gel permeation chromatography (GPC) in 1,2,4-trichlorobenzene at 135 °C (Table 2). For conventional heating, both polymers yielded comparable and moderately high molecular weights.

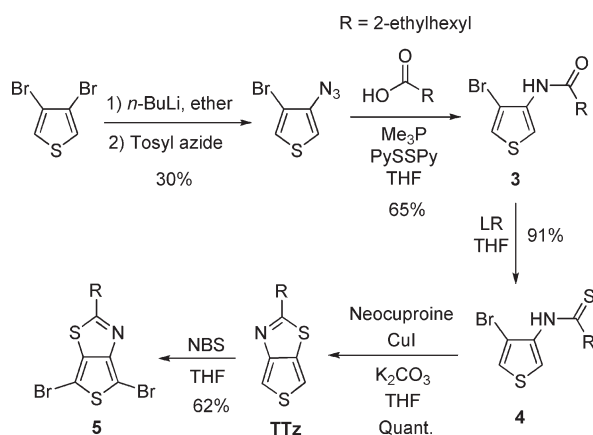
**Optical and Electrochemical Properties.** The absorption spectra and the cyclic voltammograms of the polymers are shown

in Figure 5, with all the representative data summarized in Table 3. Compared to PBnDT–TT, PBnDT–TTz exhibits a more pronounced absorption shoulder at 628 nm, indicating strong aggregation ( $\pi$ – $\pi$  stacking) in solution. However, PBnDT–TT has a broader absorption and a smaller band gap by 0.24 eV, most likely due to TT's lower resonance energy. According to DFT calculation results shown in Table 4, the difference between the band gaps of the aromatic and quinoid ester BnDT–TT is much smaller (1.33 eV) than BnDT–TTz (1.58 eV). This suggests that TT tends to favor its quinoid form more so than TTz does, leading to PBnDT–TT's smaller band gap. Nevertheless, the observed HOMO levels<sup>40</sup> (estimated by electrochemical measurement) of both polymers are identical (–5.06 eV) as the calculations predicted (Table 1), which implies that the introduction of the

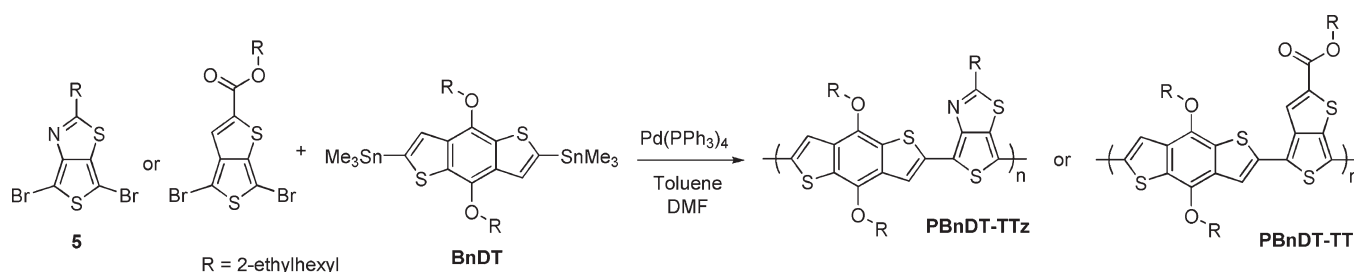
**Scheme 3. Synthesis of Thienothiazole, Procedure III, via 3-Amino-4-bromothiophene**



**Scheme 4. Synthesis of Thienothiazole, Procedure IV, via 3-Azido-4-bromothiophene**



**Scheme 5. Synthesis of Polymers (A) PBnDT–TTz and (B) PBnDT–TT**



nitrogen within the polymer backbone indeed has a similar effect on the energy levels as an ester substituent does.

**Photovoltaic Properties.** Despite having the same HOMO level, PBnDT–TTz and PBnDT–TT display vastly different PV properties (Table 5). The first major difference is the influence of the spin-casting solvent used, either chlorobenzene (CB) or *o*-dichlorobenzene (DCB). For PBnDT–TT, solvent choice made little impact on its PV properties. PCE, mobility,  $V_{oc}$ ,  $J_{sc}$  fill factor, and absorption coefficient values were all very similar in both CB and DCB (Table 5, Figures 6 and 7). Although these values differ from the polymer series reported by Liang et al.,<sup>13,14,26</sup> it is important to note that this specific side chain combination has not been reported, and it is not surprising that a slight modification in chain length would yield such a difference in PV performance.<sup>25,41,42</sup>

PBnDT–TTz, on the other hand, is greatly influenced by the processing solvent. In DCB, PV properties are inferior, especially  $J_{sc}$  and the absorption coefficient. As discussed previously, PBnDT–TTz has a stronger  $\pi$ – $\pi$  stacking ability than PBnDT–TT. Therefore, in the high boiling solvent (DCB) which extends the solvent annealing time, PBnDT–TTz chains have more time to agglomerate, detrimentally leading to further phase separation between polymer chains and PCBM molecules. This is also confirmed in the atomic force microscopy (AFM) images in which the surface morphology of PBnDT–TTz exhibits large domains in DCB (Figure 8D) compared to CB (Figure 8C). These strong agglomerations of PBnDT–TTz produce a non-uniform PBnDT–TTz/PCBM thin film processed in DCB and, consequently, a low absorption coefficient and  $J_{sc}$ . Low boiling solvent (CB) shortens annealing time and therefore reduces excessive polymer–PCBM segregation, leading to a more favorable surface morphology in the PBnDT–TTz/PCBM thin film (Figure 8C). In this initial study, AFM was used to survey the surface nature of the polymer/PCBM films which are rather thin at  $\sim 100$  nm (Table 5). However, more advanced techniques such as defocused transmission electron microscopy (TEM) or neutron scattering will be used in the future to determine the actual bulk morphology of PBnDT–TTz/PCBM films.

When processed in CB, both polymers exhibit the same  $V_{oc}$  (0.69 eV), further signifying that changing to the thiazole unit has a similar effect as substituting TT with an ester. The absence of the external ester in PBnDT–TTz case appears to have led to smaller surface domains, higher fill factor (42.4% vs 35.1%), higher  $J_{sc}$  (8.64 mA/cm<sup>2</sup> vs 4.99 mA/cm<sup>2</sup>), and higher hole

**Table 2. Polymerization Results for Polymers**

	$M_n$ [kg/mol]	$M_w$ [kg/mol]	PDI	yield [%]
PBnDT–TTz	25.7	62.6	2.43	90.3
PBnDT–TT	16.6	43.3	2.61	35.7

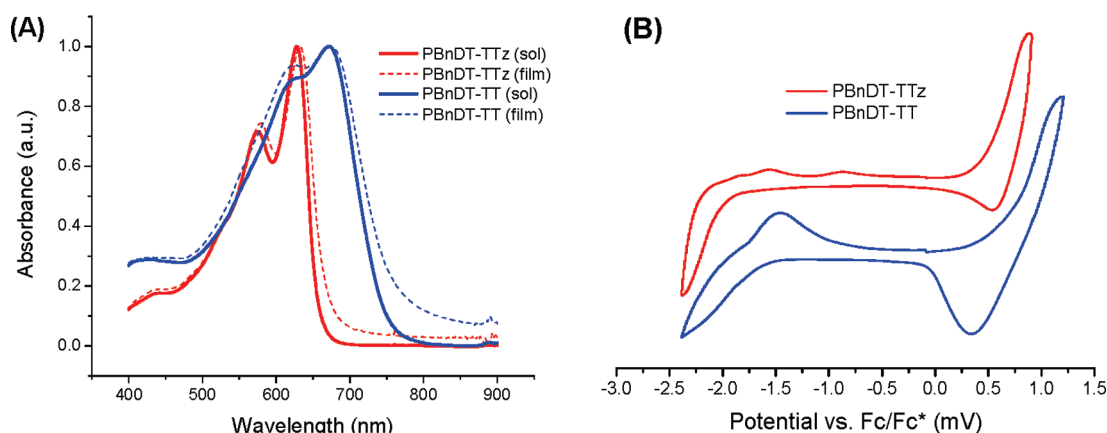


Figure 5. (A) UV-vis absorption spectra and (B) cyclic voltammograms of PBnDT-TTz and PBnDT-TT.

Table 3. Optical and Electrochemical Data of Polymers

	UV-vis absorption						cyclic voltammetry	
	CHCl <sub>3</sub> solution			film			$E_{ox,onset}$ (V)	$E_{red,onset}$ (V)
	$\lambda_{max}$ [nm]	$\lambda_{onset}$ [nm]	$E_g$ [eV]	$\lambda_{max}$ [nm]	$\lambda_{onset}$ [nm]	$E_g$ [eV]	HOMO [eV]	LUMO [eV]
PBnDT-TTz	628	658	1.88	632	670	1.85	−5.06	−2.82
PBnDT-TT	670	750	1.65	673	766	1.61	−5.06	−3.14

mobility ( $4.52 \times 10^{-5}$  vs  $2.18 \times 10^{-4}$ ), ultimately making this polymer more efficient.

## CONCLUSIONS

In summary, we have established a new synthetic route to thienothiazole, streamlining it down from seven to four much higher yielding steps. Furthermore, side-chain modification can be done much later in the synthesis, making it easier to create a library of thienothiazole-based compounds. From this new route, a new PBnDT-TTz polymer was made and compared to its TT counterpart, which is synthetically harder to produce. Both polymers exhibit the same  $V_{oc}$  and HOMO level, indicating that incorporating a nitrogen into the backbone can achieve a similar effect without sacrificing TT's beneficial qualities and eliminates the reliance on external substituents. Interestingly, PBnDT-TTz demonstrated solvent dependence, exhibiting far better surface morphology and solar cell performance in CB than in DCB. Despite having a larger band gap than its TT analogue, PBnDT-TTz's  $J_{sc}$  and mobility are considerably higher, leading to higher solar cell efficiency. These favorable results support the design motif that backbone modification can be more advantageous than an external substituent, and it also demonstrates the usefulness of the TTz moiety in photovoltaics. Furthermore, because the TTz used in this initial study has only a simple alkyl chain, other structural modifications can be made in the future to improve solar cell performance. Such studies are currently underway and will be reported in due course.

## EXPERIMENTAL SECTION

**Reagents.** 2-Azido-3-bromothiophene<sup>36</sup> was synthesized according to the literature. All solvents are ACS grade unless otherwise noted.

Table 4. DFT Calculations of Quinoid Structures for BnDT Copolymerized with Alkyl TT, Ester TT, and Alkyl TTz

	HOMO [eV]	LUMO [eV]	$E_g$ [eV]	$E_g$ difference vs aromatic [eV]
alkyl TT	−4.70	−2.94	1.76	1.55
ester TT	−4.89	−3.18	1.71	1.33
alkyl TTz	−4.78	−3.02	1.76	1.58

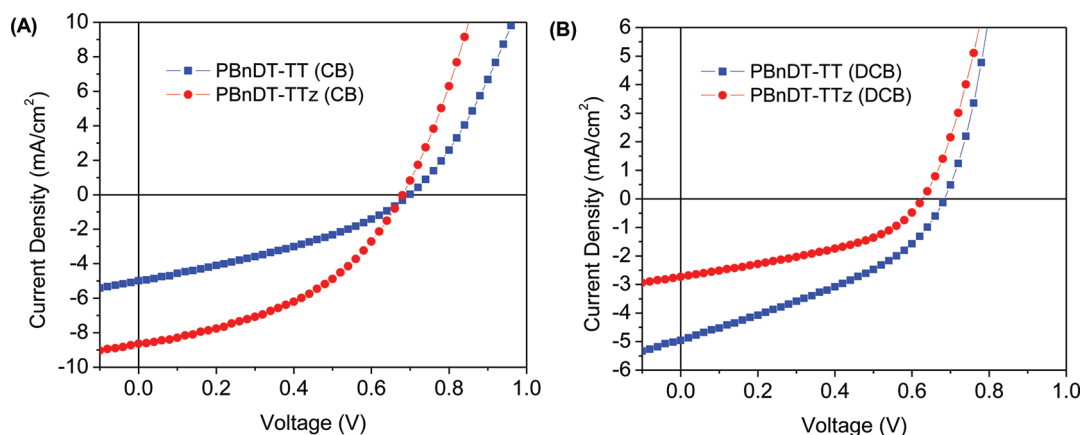
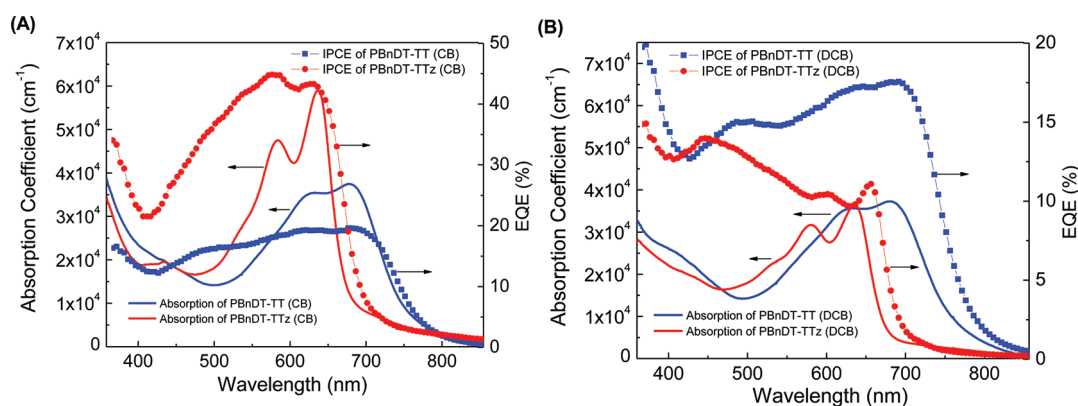
Anhydrous diethyl ether, toluene, and DMF were used as received. THF was dried by distillation from sodium/benzophenone. All other chemicals were purchased from commercial sources (Acros, Alfa Aesar, Sigma-Aldrich, Fisher Scientific, Oakwood Chemical, Matrix Scientific) and used without further purification.

**N-(4-Bromothiophenyl)-3-ethylheptanamide (3).** To a mixture of PySSPy (3.16 mmol, 0.696 g) and carboxylic acid (15.8 mmol, 2.50 g) stirring in anhydrous toluene (125 mL) under argon, 2-azido-3-bromothiophene (15.8 mmol, 3.23 g) was added. 1.0 M trimethylphosphine solution in toluene (48.7 mmol, 48.7 mL) was then slowly added at 0 °C. Reaction mixture was allowed to warm to room temperature and stirred overnight. Afterward, the mixture was extracted with saturated sodium bicarbonate and ethyl acetate. The organic layers were combined and dried over MgSO<sub>4</sub>. The compound was then purified by column chromatography by eluting with 5% ethyl acetate/hexanes to afford a colorless oil. Yield: 65%. <sup>1</sup>H NMR (CDCl<sub>3</sub>, 300 MHz,  $\delta$ ): 7.91 (d,  $J$  = 3.6 Hz, 1H), 7.23 (d,  $J$  = 3.6 Hz, 1H), 2.33 (d,  $J$  = 6.9 Hz, 2H), 1.92 (m, 1H), 1.34 (m, 8H), 0.90 (m, 6H). <sup>13</sup>C NMR (CDCl<sub>3</sub>, 400 MHz,  $\delta$ ): 170.01, 132.58, 121.22, 110.37, 104.20, 41.88, 36.91, 33.00, 28.84, 26.24, 22.92, 14.05, 10.84.

**N-(4-Bromothiophenyl)-3-ethylheptanethioamide (4).** Lawesson's reagent (15.3 mmol, 6.19 g) was added to a solution of compound (3) (10.2 mmol, 2.96 g) stirring in anhydrous THF (125 mL). The reaction mixture was refluxed overnight. Afterward, the reaction

**Table 5. Characteristic Photovoltaic Data for PBnDT–TTz and PBnDT–TT**

polymer	solvent	thickness [nm]	mobility [ $\text{cm}^2/(\text{V s})$ ]	$J_{\text{sc}}$ [ $\text{mA}/\text{cm}^2$ ]	$V_{\text{oc}}$ [V]	FF [%]	PCE [%]
PBnDT–TT	CB	105	$4.52 \times 10^{-5}$	4.99	0.69	35.1	1.2
PBnDT–TT	DCB	94	$2.22 \times 10^{-4}$	4.96	0.69	36.6	1.3
PBnDT–TTz	CB	97	$2.18 \times 10^{-4}$	8.64	0.69	42.4	2.5
PBnDT–TTz	DCB	112	$4.84 \times 10^{-4}$	2.73	0.63	41.3	0.71

**Figure 6.** Characteristic  $J$ – $V$  curves of PBnDT–TTz and PBnDT–TT BHJ solar cells in (A) chlorobenzene and (B) dichlorobenzene.**Figure 7.** Incident photon to current efficiency and solid film absorption of each blend of polymer:PC<sub>61</sub>BM in (A) chlorobenzene and (B) dichlorobenzene.

mixture was partitioned between ethyl acetate and 10% NaOH solution. The organic layer was collected and dried over  $\text{MgSO}_4$ . The mixture was then purified via column chromatography using a 5% ethyl acetate/hexanes mixture as the eluent, resulting in a pale yellow oil. Yield: 91%.  $^1\text{H}$  NMR ( $\text{CDCl}_3$ , 300 MHz,  $\delta$ ): 8.90 (d,  $J = 2.7$  Hz, 1H), 7.22 (d,  $J = 2.7$  Hz, 1H), 2.73 (d,  $J = 6.9$  Hz, 2H), 2.03 (m, 1H), 1.33 (m, 8H), 0.88 (m, 6H).  $^{13}\text{C}$  NMR ( $\text{CDCl}_3$ , 400 MHz,  $\delta$ ): 202.42, 133.67, 121.99, 114.80, 105.36, 53.92, 40.66, 32.58, 29.21, 26.06, 23.36, 14.60, 11.23.

**2-(2-Ethylhexyl)thieno[3,4-*d*]thiazole (TTz).** CuI (0.464 mmol, 88.0 mg), neocuproine (0.927 mmol, 0.193 g), and  $\text{K}_2\text{CO}_3$  (13.9 mmol, 1.92 g) were quickly added to a solution of compound (4) (9.27 mmol, 3.10 g) stirring in anhydrous THF (125 mL) under argon. The reaction mixture was then refluxed overnight and then extracted using ethyl acetate and water. Column chromatography was performed using 5% ethyl acetate/hexanes to afford a yellow oil in quantitative yield.  $^1\text{H}$  NMR ( $\text{CDCl}_3$ , 300 MHz,  $\delta$ ): 7.46 (d,  $J = 2.7$  Hz, 1H), 7.17 (d,  $J = 2.7$  Hz, 1H), 2.92 (d,  $J = 7.2$  Hz, 2H), 1.59 (m, 1H), 1.42 (m, 8H), 0.91 (m, 6H).  $^{13}\text{C}$  NMR ( $\text{CDCl}_3$ ,

400 MHz,  $\delta$ ): 178.25, 160.02, 134.29, 130.84, 109.34, 39.86, 39.60, 32.64, 28.75, 25.86, 22.93, 14.07, 10.73.

**4,6-Dibromo-2-(2-ethylhexyl)thieno[3,4-*d*]thiazole (5).** To a solution of thienothiazole (TTz) (9.67 mmol, 2.45 g) stirring in ACS grade THF (125 mL) at 0 °C, *N*-bromosuccinimide (19.34 mmol, 3.44 g) was slowly added portion-wise. The reaction mixture was then allowed to warm to room temperature and stirred overnight. After confirming by TLC that the reactant was no longer present, the mixture was then partitioned between ethyl acetate and saturated sodium bicarbonate. The combined organic layers were then dried over  $\text{MgSO}_4$ . The compound was then isolated by column chromatography using 5% ethyl acetate/hexanes, resulting in a yellow oil. Yield: 62%.  $^1\text{H}$  NMR ( $\text{CDCl}_3$ , 300 MHz,  $\delta$ ): 2.91 (d,  $J = 7.2$  Hz, 2H), 1.86 (m, 1H), 1.44 (m, 8H), 0.85 (m, 6H).  $^{13}\text{C}$  NMR ( $\text{CDCl}_3$ , 400 MHz,  $\delta$ ): 179.79, 156.75, 135.81, 128.80, 95.11, 39.93, 39.92, 32.58, 28.69, 25.86, 22.89, 14.06, 10.72.

#### Representative Stille Coupling Polymerization Procedure.

To a degassed solution of monomer (5) (0.516 mmol, 0.212 g) and

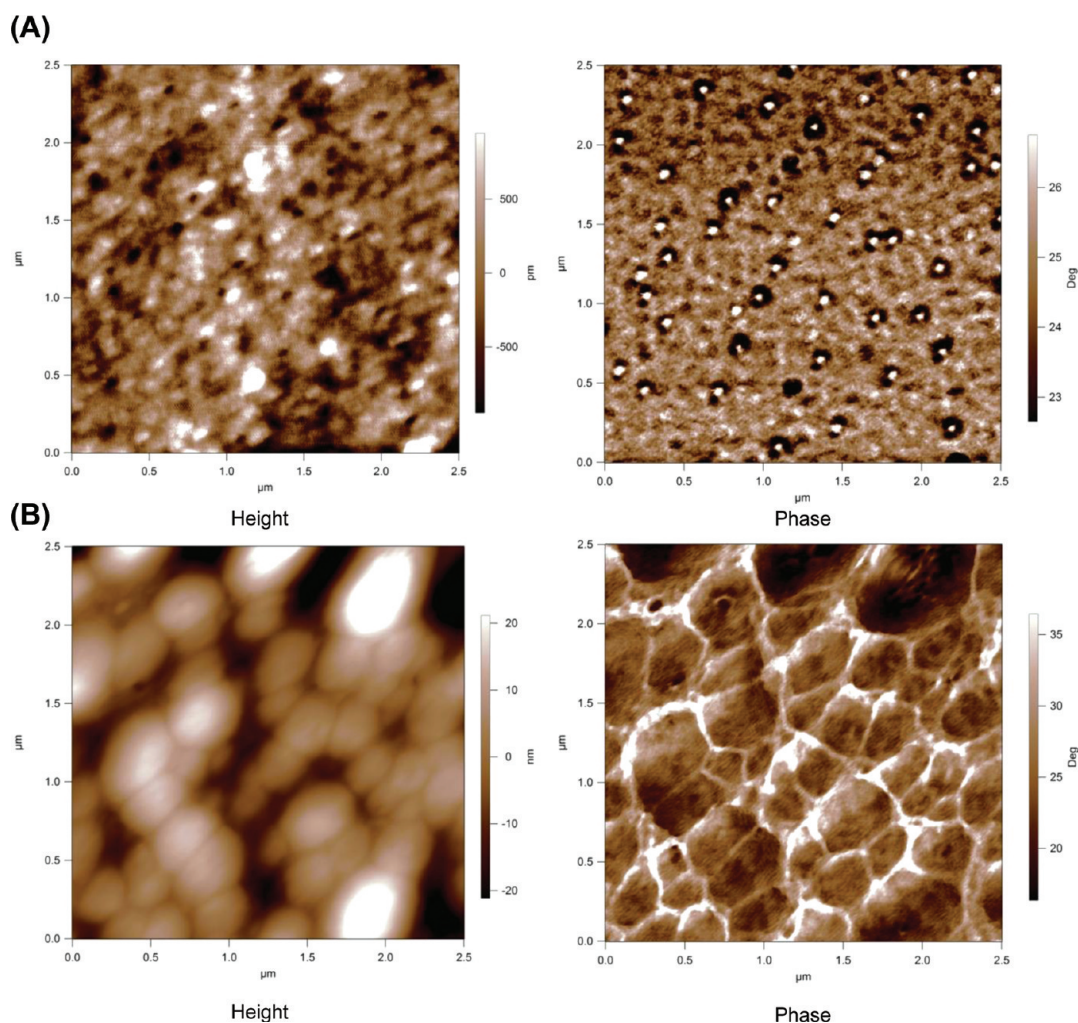


**Figure 8.** AFM images of PBnDT-TTz in (A) chlorobenzene and (B) dichlorobenzene.

distannylated benzodithiophene (0.516 mmol, 0.398 g) in anhydrous DMF (2 mL) and anhydrous toluene (8 mL) under argon, tetrakis(triphenylphosphine) palladium (0.021 mmol, 24.0 mg) was quickly added. Reaction mixture was then refluxed for 48 h. Afterward, the reaction mixture was then precipitated into methanol. The polymer solids were then collected and Soxhlet extracted with methanol, ethyl acetate, hexanes, and then chloroform. The chloroform extracts were then concentrated and precipitated into methanol and then filtered and washed with methanol. The residual solvent was then removed under vacuum, affording PBnDT-TTz as a gold-black solid.

**Instrumentation.**  $^1\text{H}$  nuclear magnetic resonance (NMR) spectra were obtained at 300 or 400 MHz as solutions in  $\text{CDCl}_3$ , 1,1,2,2-tetrachloroethane- $d_2$ , or  $\text{DMSO}-d_6$ .  $^{13}\text{C}$  NMR spectra were obtained at 100 MHz as solutions in  $\text{CDCl}_3$ . Chemical shifts are reported in parts per million (ppm,  $\delta$ ) and referenced from trimethylsilane. Coupling constants  $J$  are reported in hertz. Spectral splitting patterns are designated as s (singlet), d (doublet), m (multiplet) and br (broad). Gel permeation chromatography (GPC) measurements were carried out on a Polymer Laboratories PL-GPC 220 instrument, using 1,2,4-trichlorobenzene as the eluent (stabilized with 125 ppm BHT) at 135  $^\circ\text{C}$ . The obtained molecular weight is relative to polystyrene standards. UV-vis absorption spectra were taken by a Shimadzu UV-2401PC spectrophotometer. For the measurement of thin films, polymers were spin-coat onto precleaned glass slides from  $\sim 10$  mg/mL polymer solutions in chlorobenzene. Cyclic voltammetry measurements were performed on a

Bioanalytical Systems (BAS) Epsilon potentiostat equipped with a three-electrode configuration: a glassy carbon working electrode, a  $\text{Ag}/\text{AgNO}_3$  (0.01 M in anhydrous acetonitrile) reference electrode, and a Pt wire counter electrode. Measurements were taken under an argon atmosphere at a scan rate of 100 mV/s in anhydrous acetonitrile with tetrabutylammonium hexafluorophosphate (0.1 M) as the supporting electrolyte. Polymer films were drop cast onto the glassy carbon electrode from a concentrated polymer solution in chloroform and dried under a stream of argon prior to obtaining measurements. The potential of the  $\text{Ag}/\text{AgNO}_3$  reference electrode was internally calibrated by using the ferrocene/ferrocenium redox couple ( $\text{Fc}/\text{Fc}^+$ ). The electrochemical onsets were determined at the position where the current starts to deviate from the baseline. The highest occupied molecular orbital (HOMO) and lowest unoccupied molecular orbital (LUMO) energy levels were calculated from the onset oxidation potential ( $E_{\text{ox}}$ ) and onset reductive potential ( $E_{\text{red}}$ ), respectively, according to the following equations:

$$\text{HOMO} = -(E_{\text{ox}} + 4.8) \text{ (eV)}$$

$$\text{LUMO} = -(E_{\text{red}} + 4.8) \text{ (eV)}$$

**Polymer Solar Cell Fabrication and Testing.** Glass substrates coated with patterned tin-doped indium oxide (ITO) were purchased from Thin Film Devices, Inc. Prior to use, the substrates were cleaned via

ultrasonication in acetone, deionized water, and then 2-propanol for 20 min each. The substrates were dried under a stream of nitrogen and then treated with UV-ozone for over 30 min. A filtered dispersion of PEDOT:PSS in water (Baytron PH500) was then spun-cast onto clean ITO substrates at 4000 rpm for 60 s and then baked at 140 °C for 10 min to give a thin film with a thickness of 40 nm. Blends of polymer and PCBM (1:1 w/w, 10 mg/mL for polymers) were dissolved in corresponding solvents with heating at 120 °C for 6 h. All the solutions were filtered through a 1.0  $\mu\text{m}$  poly(tetrafluoroethylene) (PTFE) filter and spun-cast at optimized rpm for 60 s onto the PEDOT:PSS layer. The substrates were then dried at room temperature in the glovebox under a nitrogen atmosphere for 12 h. The devices were finished for measurement after thermal deposition of a 40 nm film of calcium and a 70 nm aluminum film as the cathode at a pressure of  $\sim 1 \times 10^{-6}$  mbar. There are 8 devices per substrate, with an active area of 12 mm<sup>2</sup> per device. The thicknesses of films were recorded by a profilometer (Alpha-Step 200, Tencor Instruments), and AFM Images were taken using an Asylum Research MFP3D atomic force microscope. Device characterization was carried out under AM 1.5G irradiation with the intensity of 100 mW/cm<sup>2</sup> (Oriol 91160, 300 W) calibrated by a NREL certified standard silicon cell. Current densities versus potential ( $J$ - $V$ ) curves were recorded with a Keithley 2400 digital source meter. EQE were detected under monochromatic illumination (OriolCornerstone 260 1/4 m monochromator equipped with Oriol 70613NS QTH lamp), and the calibration of the incident light was performed with a monocrystalline silicon diode. All fabrication steps after adding the PEDOT:PSS layer onto ITO substrate, and characterizations were performed in gloveboxes under a nitrogen atmosphere.

For mobility measurements, the hole-only devices in a configuration of ITO/PEDOT:PSS (40 nm)/copolymer-PCBM/Pd (50 nm) were fabricated. The experimental dark current densities  $J$  of polymer:PCBM blends were measured when applied with voltage from 0 to 6 V. The applied voltage  $V$  was corrected from the built-in voltage  $V_{\text{bi}}$  which was taken as a compensation voltage  $V_{\text{bi}} = V_{\text{oc}} + 0.05$  V and the voltage drop  $V_{\text{rs}}$  across the indium tin oxide/poly(3,4-ethylenedioxythiophene):poly(styrenesulfonic acid) (ITO/PEDOT:PSS) series resistance and contact resistance, which is found to be around 35  $\Omega$  from a reference device without the polymer layer. From the plots of  $J^{0.5}$  vs  $V$ , hole mobilities of copolymers can be deduced from the equation

$$J = \frac{9}{8} \varepsilon_r \varepsilon_0 \mu_h \frac{V^2}{L^3}$$

where  $\varepsilon_0$  is the permittivity of free space,  $\varepsilon_r$  is the dielectric constant of the polymer which is assumed to be around 3 for the conjugated polymers,  $\mu_h$  is the hole mobility,  $V$  is the voltage drop across the device, and  $L$  is the film thickness of active layer.

## ■ ASSOCIATED CONTENT

**Supporting Information.** AFM images of PBnDT-TT, DFT data, mobility data, syntheses of 3-bromothiophene-4-carboxylic acid and 3-amino-4-bromothiophene, and NMR spectra of all compounds and polymers. This material is available free of charge via the Internet at <http://pubs.acs.org>.

## ■ AUTHOR INFORMATION

### Corresponding Author

\*E-mail: [wyou@email.unc.edu](mailto:wyou@email.unc.edu).

## ■ ACKNOWLEDGMENT

This work was generously supported by a DuPont Young Professor Award, Office of Naval Research (Grant N0001411-

10235), NSF CAREER Award (DMR-0954280), and NSF Grant (CHE-1058626). We acknowledge Mr. Nabil Kleinhenz for the synthesis of 2-(2-ethylhexyl)thieno[3,4-*b*]thiophene and Prof. Richard Jordan and Mr. Nathan Contrella of the University of Chicago for GPC measurements. We also want to thank Dr. Shubin Liu of Research Computing Center at UNC Chapel Hill for DFT calculations.

## ■ REFERENCES

- (1) Brabec, C. J. *Sol. Energy Mater. Sol. Cells* **2004**, 83, 273.
- (2) Günes, S.; Neugebauer, H.; Sariciftci, N. S. *Chem. Rev.* **2007**, 107, 1324.
- (3) Thompson, B. C.; Fréchet, J. M. J. *Angew. Chem., Int. Ed.* **2008**, 47, 58.
- (4) Xiao, S.; Price, S. C.; Zhou, H.; You, W. *ACS Symp. Ser.* **2010**, 1034, 71.
- (5) Cheng, Y.-J.; Yang, S.-H.; Hsu, C.-S. *Chem. Rev.* **2009**, 109, 5868.
- (6) Coffin, R. C.; Peet, J.; Rogers, J.; Bazan, G. C. *Nature Chem.* **2009**, 1, 657.
- (7) Park, S. H.; Roy, A.; Beaupre, S.; Cho, S.; Coates, N.; Moon, J. S.; Moses, D.; Leclerc, M.; Lee, K.; Heeger, A. J. *Nature Photonics* **2009**, 3, 297.
- (8) Piliago, C.; Holcombe, T. W.; Douglas, J. D.; Woo, C. H.; Beaujuge, P. M.; Fréchet, J. M. J. *J. Am. Chem. Soc.* **2010**, 132, 7595.
- (9) Price, S. C.; Stuart, A. C.; Yang, L.; Zhou, H.; You, W. *J. Am. Chem. Soc.* **2011**, 133, 4625.
- (10) Zhou, H.; Yang, L.; Stuart, A. C.; Price, S. C.; Liu, S.; You, W. *Angew. Chem., Int. Ed.* **2011**, 50, 2995.
- (11) Chu, T.-Y.; Lu, J.; Beaupre, S.; Zhang, Y.; Pouliot, J.-R.; Wakim, S.; Zhou, J.; Leclerc, M.; Li, Z.; Ding, J.; Tao, Y. *J. Am. Chem. Soc.* **2011**, 133, 4250.
- (12) Su, M.-S.; Kuo, C.-Y.; Yuan, M.-C.; Jeng, U. S.; Su, C.-J.; Wei, K.-H. *Adv. Mater.* **2011**, 23, 3315.
- (13) Liang, Y.; Xu, Z.; Xia, J.; Tsai, S.-T.; Wu, Y.; Li, G.; Ray, C.; Yu, L. *Adv. Mater.* **2010**, 22, E135.
- (14) Liang, Y.; Feng, D.; Wu, Y.; Tsai, S.-T.; Li, G.; Ray, C.; Yu, L. *J. Am. Chem. Soc.* **2009**, 131, 7792.
- (15) Hou, J.; Chen, H.-Y.; Zhang, S.; Chen, R. I.; Yang, Y.; Wu, Y.; Li, G. *J. Am. Chem. Soc.* **2009**, 131, 15586.
- (16) Liang, Y.; Yu, L. *Acc. Chem. Res.* **2010**, 43, 1227.
- (17) Huang, Y.; Huo, L.; Zhang, S.; Guo, X.; Han, C. C.; Li, Y.; Hou, J. *Chem. Commun.* **2011**, 47, 8904.
- (18) Wakim, S.; Alem, S.; Li, Z.; Zhang, Y.; Tse, S.-C.; Lu, J.; Ding, J.; Tao, Y. *J. Mater. Chem.* **2011**, 21, 10920.
- (19) Roncali, J. *Macromol. Rapid Commun.* **2007**, 28, 1761.
- (20) Price, S. C.; Stuart, A. C.; You, W. *Macromolecules* **2010**, 43, 4609.
- (21) Zhou, H.; Yang, L.; Stoneking, S.; You, W. *ACS Appl. Mater. Interfaces* **2010**, 2, 1377.
- (22) Zhou, H.; Yang, L.; Liu, S.; You, W. *Macromolecules* **2010**, 43, 10390.
- (23) Coffin, R. C.; Peet, J.; Rogers, J.; Bazan, G. C. *Nature Chem.* **2009**, 1, 657.
- (24) Zhou, H.; Yang, L.; Xiao, S.; Liu, S.; You, W. *Macromolecules* **2010**, 43, 811.
- (25) Yang, L.; Zhou, H.; You, W. *J. Phys. Chem. C* **2010**, 114, 16793.
- (26) Liang, Y.; Wu, Y.; Feng, D.; Tsai, S.-T.; Son, H.-J.; Li, G.; Yu, L. *J. Am. Chem. Soc.* **2009**, 131, 56.
- (27) Zhou, H.; Yang, L.; Price, S. C.; Knight, K. J.; You, W. *Angew. Chem., Int. Ed.* **2010**, 49, 7992.
- (28) Kim, I. T.; Lee, J. H.; Lee, S. W. *Bull. Korean Chem. Soc.* **2007**, 28, 2511.
- (29) Pan, H.; Li, Y.; Wu, Y.; Liu, P.; Ong, B. S.; Zhu, S.; Xu, G. *J. Am. Chem. Soc.* **2007**, 129, 4112.
- (30) Pan, H.; Wu, Y.; Li, Y.; Liu, P.; Ong, B. S.; Zhu, S.; Xu, G. *Adv. Funct. Mater.* **2007**, 17, 3574.

- (31) Allard, N.; Beaupré, S.; Aïch, B. R.; Najari, A.; Tao, Y.; Leclerc, M. *Macromolecules* **2011**, *44*, 7184.
- (32) Yao, Y.; Liang, Y.; Shrotriya, V.; Xiao, S.; Yu, L.; Yang, Y. *Adv. Mater.* **2007**, *19*, 3979.
- (33) Kolb, H. C.; Finn, M. G.; Sharpless, K. B. *Angew. Chem., Int. Ed.* **2001**, *40*, 2004.
- (34) Evindar, G.; Batey, R. A. *J. Org. Chem.* **2006**, *71*, 1802.
- (35) Zhai, L.; Pilston, R. L.; Zaiger, K. L.; Stokes, K. K.; McCullough, R. D. *Macromolecules* **2002**, *36*, 61.
- (36) Spagnolo, P.; Zanirato, P. *J. Org. Chem.* **1978**, *43*, 3539.
- (37) Bures, J.; Martin, M.; Urpi, F.; Vilarrasa, J. *J. Org. Chem.* **2009**, *74*, 2203.
- (38) Bao, Z.; Chan, W. K.; Yu, L. *J. Am. Chem. Soc.* **1995**, *117*, 12426.
- (39) Carsten, B.; He, F.; Son, H. J.; Xu, T.; Yu, L. *Chem. Rev.* **2011**, *111*, 1493.
- (40) Cardona, C. M.; Li, W.; Kaifer, A. E.; Stockdale, D.; Bazan, G. C. *Adv. Mater.* **2011**, *23*, 2367.
- (41) Szarko, J. M.; Guo, J.; Liang, Y.; Lee, B.; Rolczynski, B. S.; Strzalka, J.; Xu, T.; Loser, S.; Marks, T. J.; Yu, L.; Chen, L. X. *Adv. Mater.* **2010**, *22*, 5468.
- (42) Kleinhenz, N.; Yang, L.; Zhou, H.; Price, S. C.; You, W. *Macromolecules* **2011**, *44*, 872.